Output Tracking for Actuator Deficient/Redundant Systems: Multiple Piezoactuator Example

Rob Brinkerhoff * and Santosh Devasia†
University of Utah, Salt Lake City, Utah 84112

I. Introduction

THIS Note presents an optimal-inversion-based approach to output tracking in linear, nonminimum phase systems with actuator redundancy or deficiency. Current inversion-based methods are applicable to square systems, i.e., systems with the same number of tracked outputs as the number of inputs.[1,2] In this Note we describe the extension of the inversion-based methodology to nonsquare systems, i.e., to systems with actuator redundancy or actuator deficiency; presently available inversion techniques are not applicable if the system has actuator redundancy or actuator deficiency. The proposed method can be used to allocate the output-tracking task between different actuators and can also be used to achieve tradeoffs between output tracking and other requirements such as avoiding actuator saturations. The problem is posed as the minimization of a quadratic cost functional, and the solution is developed for linear systems. The technique is illustrated by applying it to an experimental multiple-piezoactuator system.

Actuator redundancy occurs, for example, when a low-bandwidth, large-range actuator is supplemented with a high-bandwidth (potentially low-range) actuator to achieve large-range high-bandwidth actuation. For example, micromanipulators have been added to the tips of large (macro) flexible manipulators to provide additional high-bandwidth manipulation capability (see, for example, Ref. 3). For such actuator-redundant systems a systematic approach is needed to allocate a given output-tracking task between the different actuators. Such a distribution of tracking efforts is also needed for output tracking in actuator-deficient systems where exact tracking of all of the output trajectories may not possible when the number of outputs is more than the number of inputs. Actuator deficiency occurs in flexible manipulators and aerospace applications where requirements like vibration reduction are added to typical goals like endpoint tracking (see, for example, Ref. 4). For such actuator-deficient and actuator-redundant systems there is a need to develop systematic approaches to specify and achieve tradeoffs in output tracking.

An inversion-based approach for actuator-redundant (macro-micro actuation) systems has been proposed in Ref. 3 in which a feedback controller is used for the macropart and an inversion-based controller is designed for the micropart. A similar methodology has been proposed by Yim and Singh,[5] who investigate the design of a predictive controller, which steers the endpoint of the macromanipulator with minimal vibrations, and then uses an inversion-based controller for the micropart to achieve precise end-effector control. Inversion-based approaches have also been developed for the nonlinear actuator redundant case using pseudoinversion approaches (see, for example, Ref. 6). Such inversion-based approaches attempt to exploit the known dynamics of the system to achieve precision output tracking. When the microactuator is colocated at the controlled-output point (usually, the tip of the manipulator), the dynamics between the microactuator input and the controlled output is minimum phase, and standard inversion techniques can be applied. However, inversion for general actuator-redundant systems (with potentially nonminimum phase dynamics) is challenging because standard approaches to inversion can lead to unbounded inputs. Recently developed stable-inversion techniques resolve this problem of unbounded inverse inputs by finding bounded (but possibly noncausal) input-state trajectories.[1,2] The noncausality of the inputs found by inversion can be accommodated by using preview-based controllers,[7] which enables the online specification of the desired outputs. Currently available inversion-based methods are, however, applicable to square systems. In this Note, the output tracking problem for nonsquare systems is posed as the optimization of a general quadratic cost functional and is solved in the context of linear systems. The resulting design procedure can also be used to obtain tradeoffs between the output-tracking requirement and other requirements such as reductions in input magnitudes. This extension of currently available inversion methodologies to nonsquare linear systems is described in the current Note. In Sec. II, the optimal-inversion problem is posed, and a solution is given for a general multi-input multi-output (MIMO) system. In Sec. III, the approach is applied to a multiple piezoactuator system, and experimental results are presented.

II. Problem Formulation and Solution

In this section we pose the optimal-inverse problem as the minimization of a quadratic cost functional and solve it in the context of linear time-invariant systems. We begin with the inversion problem for square systems and then pose the optimal output tracking problem for nonsquare systems.

A. Optimal Output Tracking Problem

Consider a linear time-invariant MIMO system, with its dynamics described by

$$\dot{x}(t) = Ax(t) + Bu(t), \qquad y(t) = Cx(t) \tag{1}$$

where $x \in \boldsymbol{R}^k$ is the states, the number of inputs is $n (u \in \boldsymbol{R}^n)$, and the number of outputs is $m (y \in \boldsymbol{R}^m)$. The assumption is made that this system is stable or has been stabilized with feedback (i.e., matrix A is Hurwitz). The output $y(\cdot)$ can be written in the frequency domain as $y(j\omega) = C(j\omega I - A)^{-1}Bu(j\omega) \triangleq G(j\omega)u(j\omega)$, where $G(j\omega) \in \boldsymbol{C}^{m\times n}$ represents the system's transfer-function matrix. If the system has the same number of inputs as outputs (square system), then we can find the control inputs (u_{ff}) that exactly track a desired output trajectory y_d from system inversion as in Ref. 1

$$u_{ff}(j\omega) = G(j\omega)^{-1}y_d(j\omega)$$

This input u_{ff} leads to a bounded, exact-tracking, input trajectory if the desired output $[y_d(\cdot)]$ and a certain number of its time derivatives are bounded and if the system's internal dynamics is hyperbolic.[2] This method is, however, applicable to square systems. If the number of inputs is more than the number of outputs ($n > m$), then the system is actuator redundant, and the exact-tracking inputs are not unique. If the number of inputs is less than the number of outputs ($n < m$), then the system is actuator deficient, and exact-output tracking of all of the outputs cannot be achieved for general output trajectories. For actuator-redundant and actuator-deficient systems the goal is to find an optimal input u_{opt} that achieves the best allocation of control inputs to achieve tracking of the desired output trajectories. We pose this problem as the minimization of the following quadratic performance index:

$$J(u) = \int_{-\infty}^{\infty} \Big\{ u^*(j\omega)R(j\omega)u(j\omega) + [y(j\omega) - y_d(j\omega)]^*Q(j\omega)[y(j\omega) - y_d(j\omega)] \Big\}\, d\omega \tag{2}$$

where $*$ denotes the conjugate transpose of matrices with complex elements, $R(j\omega)$ and $Q(j\omega)$ represent the weights on the input- and the output-tracking error respectively, and y_d is the desired output trajectory specified by the user. If the weight R on the input is chosen as zero, then the minimization of the performance index will lead to the exact-tracking inputs found by inverting the system (if the output trajectories are sufficiently smooth, the system is square, and the internal dynamics is hyperbolic.[2]) Thus, the performance index is a generalization of the inversion problem to nonsquare systems. A

Received 17 June 1999; revision received 5 October 1999; accepted for publication 6 October 1999.

*Graduate Research Assistant, Department of Mechanical Engineering, MEB 3201, 50 South, Central Campus Drive; currently, GNC Engineer, M/S M7, Raytheon Systems, 1151 East Hermes Road, Building 807, Tucson, Arizona 85706; rbrinkerhoff@west.raytheon.com.

†Assistant Professor, Department of Mechanical Engineering, MEB 3201, 50 South, Central Campus Drive; santosh@eng.utah.edu.

similar frequency-dependent quadratic performance index has been used in the past (e.g., Ref. 8) for system regulation ($y_d = 0$); however, such approaches were aimed at finding causal control laws. In contrast, we allow, in the following, noncausal solutions to the optimal-inversion problem—these noncausal solutions can be implemented using preview-based approaches.[7] In summary, given a Fourier-transformable desired output trajectory, the optimal inversion-based output tracking problem is stated as the minimization of the cost functional J over all Fourier-transformable inputs, $\min_u J(u)$.

The focus of this Note is to solve this minimization problem for a general cost functional and leave the choice of the weighting matrices, Q and R in Eq. (2), to the designer (as in current linear-quadratic-optimal-control literature). For example, tradeoffs between tracking different output trajectories (in actuator deficient systems) can be designed by choosing different output-tracking error weightings Q in Eq. (2). Similarly, the cost function can be used to account for different actuator bandwidths and ranges in actuator-redundant systems by choosing different control weightings, R. Thus, the output-tracking requirements can be specified by varying the matrices Q and R. These choices in weightings will be illustrated in Sec. III.

B. Solution to the Optimal Output Tracking Problem

The optimal output-tracking control law, found by the minimization of the performance index (2), is given by the following lemma.

Lemma: Let Q and R in the performance index (2) be symmetric, positive-semidefinite, real matrices, and let $\Lambda(j\omega) \triangleq R(j\omega) + G^*(j\omega)Q(j\omega)G(j\omega)$. Then, the optimal input trajectory u_{opt} that minimizes the performance index (2) is given by

$$u_{\text{opt}}(j\omega) = \Lambda^+(j\omega)G^*(j\omega)Q(j\omega)y_d(j\omega) \tag{3}$$

$\Lambda^+(j\omega)$ is the pseudo (generalized) inverse[9] of $\Lambda(j\omega)$ and U; Σ (invertible) and V define the singular value decomposition of Λ as $\Lambda = U[\text{diag}(\Sigma \quad 0)]V^*$. We also define $\Lambda^+(j\omega) = 0$ if $\Lambda(j\omega) = 0$ and note that $\Lambda^+(j\omega) = \Lambda^{-1}(j\omega)$ if $\Lambda(j\omega)$ is invertible.

Proof: The performance index (2) is minimized with respect to u if the quadratic term inside the integral is minimized at each $j\omega$: this nonnegative term can be rewritten as

$$I[u(j\omega)] \triangleq u(j\omega)^*\Lambda(j\omega)u(j\omega) - 2y_d^*(j\omega)Q(j\omega)G(j\omega)u(j\omega) + y_d^*(j\omega)Q(j\omega)y_d(j\omega) \tag{4}$$

The result follows the optimization of quadratic, matrix functions because $I[u(j\omega)]$ is nonnegative (see Ref. 9, Chapter 4, Theorem 4.2.1, for a detailed proof). □

In the preceding lemma the requirements on the weighting matrices Q and R can be changed from real-symmetric matrices to Hermitian matrices.[9] When the optimal input u_{opt} is applied to the system, the resulting output trajectory y_{opt} can be found as

$$\begin{aligned} y_{\text{opt}}(j\omega) &= G(j\omega)u_{\text{opt}}(j\omega) \\ &= G(j\omega)\Lambda^+(j\omega)G^*(j\omega)Q(j\omega)y_d(j\omega) \triangleq G_f(j\omega)y_d(j\omega) \end{aligned} \tag{5}$$

Thus, $G_f(j\omega)$ represents a filter that modifies the desired output trajectory $y_d(j\omega)$. The tracking error e caused by output modification can be quantified using the output filter as

$$\|e(\cdot)\|_2 = \|1 - G_f(\cdot)\|_\infty \|y_d(\cdot)\|_2$$

where $\|\cdot\|_2$ is the standard L_2 norm and $\|\cdot\|_\infty$ is the L_2-induced norm (see, e.g., Ref. 10, Sec. 4.5). The approach finds the optimal control law u_{opt}, which exactly tracks the modified output trajectory y_{opt}. This control law can be noncausal, but can be implemented using a preview-based approach.[7]

III. Multiple Piezoactuator Example

An experimental system designed to emulate dual-actuator redundant systems studied in the past (e.g., Ref. 3) is shown in Fig. 1. It has a large-range actuator that provides the main actuation with a short-range actuator attached to the end of the large-range actuator. The two inputs to the system are the voltages applied to these two piezoactuators. The large-range actuator is used to achieve most of the low-frequency actuation; it is called the low-frequency actuator (LFA). Similarly, the short-range piezo at the tip is mainly used for high-frequency actuation; it is called the high-frequency actuator (HFA). In the following, two outputs of the system will be considered. One output is the displacement at the endpoint of the dual-piezo system y_e, and the other output is the displacement of the midpoint y_m, as shown in Fig. 1; the outputs are measured using an inductive sensor. These measurements are not used for feedback-based control in the current article because our goal is to illustrate the optimal-inversion-based output-tracking approach. Therefore, only the inputs found from the optimal-inversion approach are used as feedforward control, and feedback control is not used. Feedback control can, however, be added (to the feedforward approach) to reject errors caused by external disturbances and modeling discrepancies.

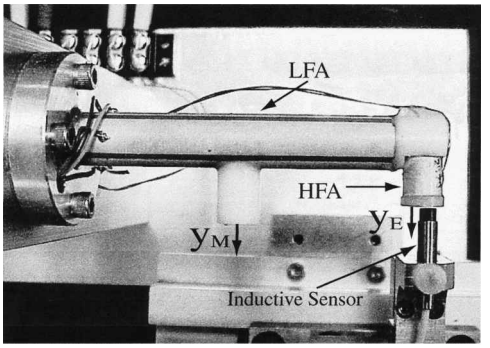

Fig. 1 Experimental piezoactuator system.

Models for two cases were obtained: an actuator-redundant case and an actuator-deficient case. For the actuator-deficient case, the voltage u_l applied to the LFA is considered as the input, and the displacements (y_m and y_e) are the outputs. The actuator-deficient system equation can be expressed as

$$\begin{bmatrix} y_m(j\omega) \\ y_e(j\omega) \end{bmatrix} = \begin{bmatrix} g_{\text{lm}}(j\omega) \\ g_{\text{le}}(j\omega) \end{bmatrix} u_l(j\omega) \tag{6}$$

For the actuator-redundant case the inputs are the voltages applied to the piezoactuators (u_h, u_l), and the output is the displacement at the endpoint y_e. The actuator-redundant system can be expressed as

$$y_e(j\omega) = g_{\text{he}}(j\omega)u_h(j\omega) + g_{\text{le}}(j\omega)u_l(j\omega) \tag{7}$$

The transfer functions (g_{lm}, g_{le}, and g_{he}) given by $g_i(j\omega) = n_i(j\omega)/d(j\omega)$ for i belonging to the set {lm, le, he} were obtained experimentally using a dynamic signal analyzer and can be represented as

$$\begin{aligned} d(j\omega) &= (j\omega + 126 \pm j4.42k)(j\omega + 1.3k \pm j12.57k) \\ &\quad \times (j\omega + 1.9k \pm j24.82k)(j\omega + 970 \pm j30.28k) \\ &\quad \times (j\omega + 21.5k \pm j63.58k) \\ n_{(\text{le})}(j\omega) &= -184e^6(j\omega + 62.83k)(j\omega - 21.34k) \\ &\quad \times (j\omega + 886 \pm j11.97k)(j\omega + 1.13k \pm j21.26k) \\ &\quad \times (j\omega - 741 \pm j30k) \\ n_{(\text{lm})}(j\omega) &= -294e^6(j\omega - 6.283k)(j\omega + 11.31k) \\ &\quad \times (j\omega + 1.59k \pm j13.09k)(j\omega - 9.42k \pm j33.3k) \\ &\quad \times (j\omega - 443 \pm j26.39k) \\ n_{(\text{he})}(j\omega) &= 84.68e^6(j\omega + 132 \pm j4.84k)(j\omega + 767 \pm j11.75k) \\ &\quad \times (j\omega + 2.56k \pm j27k)(j\omega + 823 \pm j30.85k) \end{aligned}$$

A. Actuator-Redundant and Actuator-Deficient Cases

Next, we describe the application of the optimal inversion methodology to two cases: an actuator-redundant case and an

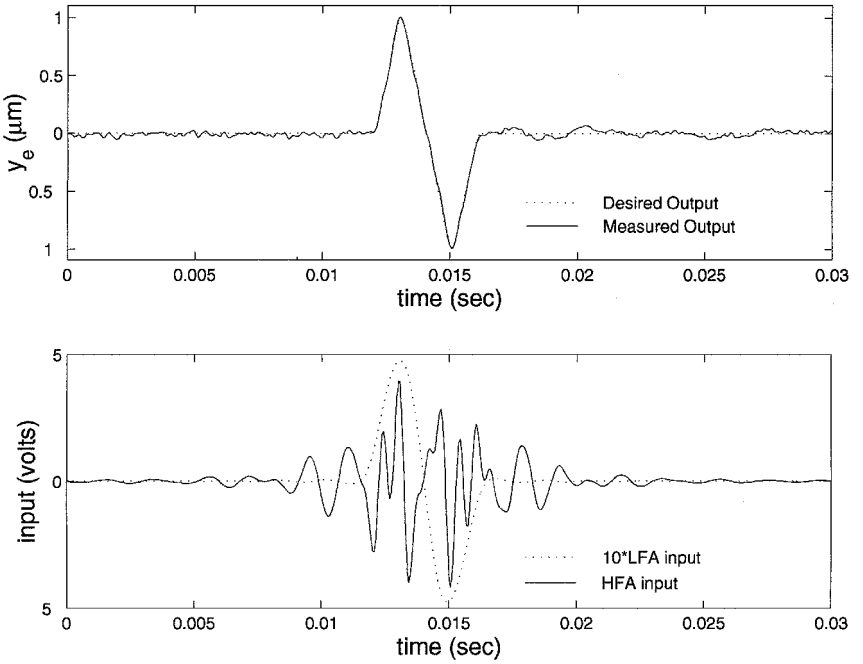

Fig. 2 Experimental results for redundant-actuator case: tracking a 250-Hz triangular output.

actuator-deficient case. For the two-input (u_l and u_h) one-output (y_e) actuator-redundant system, which is described by Eq. (7), the form of the weighting matrices were chosen as $Q(j\omega) = q_e(j\omega)$ the weighting on the output-tracking error, and $R(j\omega) = \text{diag}[r_l(j\omega)\ \ r_h(j\omega)]$, where r_l is the weighting on the input to the LFA and r_h is the weighting on the input to the HFA. The optimal inputs $u_{l_{\text{opt}}}$ and $u_{h_{\text{opt}}}$ can be found explicitly as (when the matrix Λ in the lemma is invertible and therefore pseudoinversion is not needed)

$$u_{l_{\text{opt}}} = \frac{q_e r_h g^*_{\text{le}}}{r_l r_h + q_e r_l g^*_{\text{he}} g_{\text{he}} + q_e r_h g^*_{\text{le}} g_{\text{le}}} y_{ed}$$

$$u_{h_{\text{opt}}} = \frac{q_e r_l g^*_{\text{he}}}{r_l r_h + q_e r_l g^*_{\text{he}} g_{\text{he}} + q_e r_h g^*_{\text{le}} g_{\text{le}}} y_{ed} \tag{8}$$

where y_{ed} is the desired output displacement at the endpoint and the explicit dependence on $j\omega$ is not written for ease in notation.

For the one-input (u_l) two-output (y_e and y_m) actuator-deficient system described by Eq. (6), the weighting matrices were chosen to be of the form $Q(j\omega) = \text{diag}[q_{\text{lm}}(j\omega)\ \ q_{\text{le}}(j\omega)]$ and $R(j\omega) = r(j\omega)$. It is not possible to track the two outputs at the endpoint and the midpoint with a single input. Thus, some of the desired output tracking of the endpoint displacement y_e must be traded to achieve reductions in the midpoint displacement y_m. However, such a tradeoff is not necessarily just a scaling down of the desired endpoint trajectory, and the methodology provides a design tool to specify and achieve a desired tradeoff. In the performance index q_{lm} is the weighting on the midpoint displacements, q_{le} is the weighting on the endpoint tracking error, and r is the weighting on the input to the piezoactuator (LFA). If the invertibility condition on Λ in the lemma is satisfied (e.g., if r is nonzero), then the control law can be written as

$$u_{\text{opt}} = \frac{q_{\text{le}} g^*_{\text{le}}}{r + q_{\text{lm}} g^*_{\text{lm}} g_{\text{lm}} + q_{\text{le}} g^*_{\text{le}} g_{\text{le}}} y_{d_e} + \frac{q_{\text{lm}} g^*_{\text{lm}}}{r + q_{\text{lm}} g^*_{\text{lm}} g_{\text{lm}} + q_{\text{le}} g^*_{\text{le}} g_{\text{le}}} y_{d_m} \tag{9}$$

where y_{d_m} and y_{d_e} are the desired output trajectories at the midpoint and at the endpoint of the LFA piezoactuator.

B. Experimental Results and Discussion

For brevity, we only present experimental results for the actuator redundant case. Detailed simulation and experimental results can be found in Ref. 11. For the actuator-redundant case the LFA was used for tracking low-frequency components of a desired output (shown in Fig. 2); the LFA-input's weighting r_l was, therefore, set to zero on the interval 0–300 Hz. The HFA was used to track the high-frequency components; thus, the HFA-input's weighting r_h was set to a relatively small value of 10^{-4} (compared to the weighting r_l on the LFA input) for frequencies between 500 Hz and 2.2 kHz. In the experiments the weight on the output-tracking error q_e was set to a large number (10^3, which was large relative to the weights on the inputs) on the interval 0–2.2 kHz to achieve high-precision output tracking in this frequency range. After 2.25 kHz the system model was less accurate,[11] and, therefore, the weight on the output-tracking error q_e was set to zero beyond 2.25 kHz (with r_l and r_h nonzero). These choices of weights illustrate the use of the methodology to design the allocation of the tracking task between different actuators. For example, the relatively low weights for the HFA inputs in the high-frequency range resulted in the HFA being used, primarily, to control the high-frequency components in the output trajectory as shown in Fig. 2. Similarly, the magnitude of the input weights (r_l and r_h) can also be increased, relative to the weight on the output-tracking error q_e, to avoid actuator saturation.

IV. Conclusion

A technique to achieve output tracking for linear systems with redundant/deficient actuators was presented. This approach provides a systematic method to optimally allocate output-tracking tasks between redundant actuators and to design tradeoffs in output-trajectory tracking when the number of inputs is fewer than the number of outputs (i.e., actuator-deficient systems). The methodology was illustrated by applying it to a multiple piezoactuator-based system, and experimental results were presented.

Acknowledgments

Financial support from NSF Grants CMS 9813080 and DMII 9612300 are gratefully acknowledged.

Reference

[1] Bayo, E., "A Finite-Element Approach to Control the End-Point Motion of a Single-Link Flexible Robot," *Journal of Robotic Systems*, Vol. 4, No. 1, 1987, pp. 63–75.

[2] Devasia, S., Chen, D., and Paden, B., "Nonlinear Inversion-Based Output Tracking," *IEEE Transactions on Automatic Control*, Vol. 41, No. 7, 1996, pp. 930–943.

[3] Yoshikawa, T., Hosoda, K., Doi, T., and Murakami, H., "Dynamic Trajectory Tracking Control of Flexible Manipulator by Macro-Micro Manipulator System," *Proceedings of IEEE International Conference on Robotics and Automation*, Vol. 3, IEEE Computer Society Press, Los Alamitos, CA, May 1994, pp. 1804–1809.

[4] Dewey, J., Leang, K., and Devasia, S., "Experimental and Theoretical

Results in Output-Trajectory Redesign for Flexible Structures," *Journal of Dynamic Systems, Measurement, and Control*, Vol. 120, No. 4, 1998, pp. 456–461.

[5]Yim, W., and Singh, S. N., "Nonlinear Inverse and Predictive End Point Trajectory Control of Flexible Macro-Micro Manipulators," *Journal of Dynamic Systems, Measurement, and Control*, Vol. 119, No. 3, 1997, pp. 412–420.

[6]Snell, S. A., Enns, D. F., and Garrad, W. L., Jr., "Nonlinear Inversion Flight Control for a Supermaneuverable Aircraft," *Journal of Guidance, Control, and Dynamics*, Vol. 15, No. 4, 1992, pp. 976–984.

[7]Zou, Q., and Devasia, S., "Preview-Based Stable-Inversion for Output Tracking," *Journal of Dynamic Systems, Measurement, and Control*, Vol. 121, No. 4, 1999, pp. 625–630.

[8]Gupta, N. K., "Frequency Based Cost Functions: Extensions to Linear-Quadratic-Gaussian Design Methods," *Journal of Guidance and Control*, Vol. 3, No. 6, 1980, pp. 529–535.

[9]Ortega, J. M., *Matrix Theory: A Second Course*, Plenum, New York, 1987, pp. 151–154.

[10]Zhou, K., Doyle, J. C., and Glover, K., *Robust and Optimal Control*. Prentice–Hall, Upper Saddle River, NJ, 1996, pp. 104–110.

[11]Brinkerhoff, R., "Output Tracking in Actuator Deficient/Redundant Systems: Theoretical and Experimental Results," M.S. Thesis, Mechanical Engineering Dept., Univ. of Utah, Salt Lake City, UT, Dec. 1999.

Flight Control Design of an Automatic Landing Flight Experiment Vehicle

Atsushi Fujimori* and Munerou Kurozumi†
Shizuoka University,
3-5-1 Johoku, Hamamatsu 432-8561, Japan
and
Peter N. Nikiforuk‡ and Madan M. Gupta§
University of Saskatchewan,
Saskatoon, Saskatchewan S7N 5A9, Canada

I. Introduction

THE National Aerospace Laboratory (NAL) and the National Aerospace Development Agency (NASDA) in Japan have been developing an unmanned reentry space vehicle, named HOPE-X, for a decade.[1] An Automatic Landing Flight Experiment vehicle called ALFLEX, which is a 37%-sized model of the HOPE-X, has been studied to develop an automatic landing control system. To implement a reliable automatic control system on the HOPE-X, several control design techniques have been proposed.[2–5] Sunazawa and Ohta[3] used the inverse dynamics transformation to compensate the nonlinearity of the ALFLEX. Miyajima and Kuze[4] applied neural networks to navigate the ALFLEX a reference trajectory. The NAL/NASDA designed a guidance and control law using multiple delay models and a multiple design points method.[5]

This Note presents an alternative flight control design of the ALFLEX using a fuzzy gain-scheduling (FGS) state-feedback technique in the frame of a double-loop control system (DLCS). The DLCS consists of the inner and the outer loops that are used for stabilizing the controlled system and tracking the command, respectively. In this Note, an inner-loop controller is designed by the FGS state-feedback technique[6] to guarantee the stability over the entire operating range of the ALFLEX, whereas the outer-loop controller is designed so as to improve the tracking property. The proposed control design method is applied to a numerical simulation program for an automatic landing test of the ALFLEX[2] to evaluate control performance of the designed control law.

Received 30 March 1999; presented as Paper 99-4057 at the AIAA Guidance, Navigation, and Control Conference, Portland, OR, 9–11 August 1999; revision received 7 October 1999; accepted for publication 7 October 1999.

*Associate Professor, Department of Mechanical Engineering; a-fujimori@eng.shizuoka.ac.jp.
†Graduate Student, Department of Mechanical Engineering.
‡Dean Emeritus, Department of Mechanical Engineering.
§Professor, Department of Mechanical Engineering.

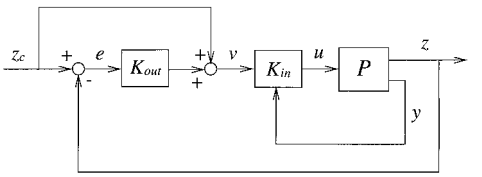

Fig. 1 Double loop control system.

II. Double-Loop Control System

Figure 1 shows a block diagram of a DLCS applying to the ALFLEX. z is the controlled variable, z_c is its command input, y is the feedback variable, u is the control input, and v is the inner-loop command input. P is a controlled plant, K_{in} is an inner-loop controller, and K_{out} is an outer-loop controller. The ALFLEX is an unstable controlled plant, and contains nonlinear factors and uncertainties. The control system for the ALFLEX therefore, should be designed not only to stabilize, but also to compensate for tracking error $e \triangleq z_c - z$ due to the nonlinear factors and uncertainties. Then, the inner loop is used for augmenting the stability of the system, whereas the outer loop is used for reinforcing the tracking property.

Now, let us discuss the outer loop of Fig. 1 using linear transfer functions. Let T_{zv} be a transfer function from v to z. A transfer function from z_c to z, T_{zz_c} is then written as

$$T_{zz_c} = (I + T_{zv}K_{\text{out}})^{-1}T_{zv}(I + K_{\text{out}}) \tag{1}$$

If K_{in} is designed so as to stabilize the controlled plant and satisfy $T_{zv}(0) = I$, the steady-state of z for a step command z_c is given by

$$z(\infty) = \lim_{s \to 0} sT_{zz_c}(s)(1/s)z_c = z_c \tag{2}$$

The servo condition, $z(\infty) = z_c$, is always satisfied. Then, K_{out} is designed so as to stabilize T_{zv} and improve the tracking property of T_{zz_c}.

III. Inner-Loop Design Using FGS State-Feedback

This section describes a design of the inner-loop controller using a FGS state-feedback technique.[6] A controlled plant considered in this study is given by the following nonlinear system:

$$\dot{x}(t) = f[x(t), u(t)], \qquad z(t) = g[x(t), u(t)] \tag{3}$$

where $u(t)$, $z(t)$, and $x(t)$ are m-dimensional input, p-dimensional controlled variable, and n-dimensional state vectors, respectively. It is assumed that $x(t)$ is available for feedback; that is, $y(t) = x(t)$ in Fig. 1.

Over the operating range of the system, let us select r linearized points (x_i^d, u_i^d) $(i = 1, \ldots, r)$ and construct a linear time-invariant (LTI) model for each linearized point. Let η_j $(j = 1, \ldots, g)$ be variables that recognize the linearized points, and N_{ji} $(i = 1, \ldots, r)$ be fuzzy sets of η_j. Fuzzy rules representing a nonlinear system [Eq. (3)] is given as follows:

If $\eta_1 = N_{1i}$ and $\cdots$ and $\eta_g = N_{gi}$, then the nonlinear system Eq. (3) is approximated by

$$\begin{bmatrix} \dot{x}(t) \\ z(t) \end{bmatrix} = \begin{bmatrix} A_i & B_i \\ C_i & D_i \end{bmatrix} \begin{bmatrix} x(t) - x_i^d \\ u(t) - u_i^d \end{bmatrix} + \begin{bmatrix} 0 \\ z^d \end{bmatrix}, \qquad (i = 1, \ldots, r) \tag{4}$$

where

$$A_i \triangleq \frac{\partial f(x_i^d, u_i^d)}{\partial x^T}, \qquad B_i \triangleq \frac{\partial f(x_i^d, u_i^d)}{\partial u^T}$$

$$C_i \triangleq \frac{\partial g(x_i^d, u_i^d)}{\partial x^T}, \qquad D_i \triangleq \frac{\partial g(x_i^d, u_i^d)}{\partial u^T}$$